Torque measurements from MW wind turbine Gearboxes

A system identification approach

Santiago, U. Gutierrez; Van Wingerden, J. W.; Polinder, H.; Sisón, A. Fernández

Important note
To cite this publication, please use the final published version (if applicable).
Please check the document version above.

Torque measurements from MW wind turbine Gearboxes: a system identification approach

View the article online for updates and enhancements.

Torque measurements from MW wind turbine Gearboxes: a system identification approach

U Gutierrez Santiago[1,2], J W van Wingerden[1], H Polinder [1], A Fernández Sisón [2]

[1] TU Delft 3mE, Mekelweg 2, 2628 CD Delft, The Netherlands
[2] Siemens Gamesa, Parque Tecnologico de Bizkaia, 48170 Zamudio, Spain

E-mail: `u.gutierrezsantiago@tudelft.nl`

Abstract. The gearbox is a critical component of modern MW wind turbines. An accurate model of the gearbox dynamics is needed to improve gearbox design, develop advanced control algorithms, and more effective fault diagnosis tools which could lead to lower the cost of energy from wind. The objective of this paper is to investigate how torque measurements can be used in a data-driven framework to build dynamic models of wind turbine gearboxes.

An initial torsional model has been derived from first principles considering the stiffness of the gears, shafts, and structural components in the gearbox together with the mechanical components of the test bench. This model has been used to create simulated data of the experiments performed on gearboxes and to apply system identification techniques to the simulated signals, with a focus on predictor based subspace identification methods. System identification has been applied to torque and speed data measured on physical tests of two 3.4MW gearboxes. Gearbox excitation frequencies and their harmonics dominate the measured signals and disturb the system identification algorithms. Several techniques have been investigated to remove the shaft rotation and gear mesh frequency harmonics of the torque and rotational speed signals based on time synchronous averaging.

1. Introduction

The cost of energy has become the critical driver for wind energy research. Nowadays, 75% of onshore wind turbines have a gearbox [12], and the gearbox is one of the main contributors to capital expenditure of onshore wind energy projects. Gearbox reliability is improving, but gearboxes continue to be the largest source of wind turbine downtime and generally do not reach the desired design life of 20 years [3]. Improvements in gearbox technology could, therefore, lead to a significant reduction in the cost of energy from wind. Three main applications are sought from data-driven models: improve gearbox design, develop advanced control algorithms, and more effective fault diagnosis tools, which would, in turn, lower the cost of energy.

It is widely acknowledged that there is a lack of knowledge of sub-systems interaction and the effect of the control strategy on the gearbox behaviour [12]. The mechanical flexibility of the gearbox and other drive train components do influence the global dynamic behaviour of the wind turbine, and this influence is not included in traditional engineering models [2]. Complex physically derived models have been created to study gearbox dynamics but have not been used together with whole turbine models, and thus traditional wind turbine design codes lack insight into the dynamic behaviour of the internal drive train components [7]. To find the best trade-

off, accurate judgment about the required model complexity is necessary. Historically, model validation has been limited because, in reality, it is complicated to get measurement data.

A data-driven modelling methodology is proposed to improve the assessment of the remaining useful life of the gearbox components and develop novel operating concepts. When these models are used for control purposes, control performance is tied directly to the accuracy of the identified model [9]. The whole drivetrain of a WT can be considered as a controlled electromechanical system with non-deterministic excitation [10] operated under closed-loop feedback control. Increasing the integration of condition monitoring systems with control functions would enable the deployment of advanced operation and maintenance concepts. This paper explores what information about the gearbox dynamics can be extracted from the torque signals in a back-to-back gearbox test bench, to achieve data-driven models of the gearbox.

The remainder of this paper is organized as follows: Section 2 gives background information on the gearboxes used for this study. Section 3 describes an initial torsional model derived from first principles taking into account the stiffness of the gears, planet carriers and housings of the gearbox. Section 4 shows the data gathered during the tests performed with two gearboxes in a back to back test bench. Initial system identification results and different techniques for harmonic removal are discussed in Section 5. Section 6 draws the main conclusions of this work and recommendations for future work.

2. Background
2.1. SGRE 3.X Gearbox
The primary purpose of the main gearbox in a wind turbine is to transfer the torque from the rotor to the generator handling the increase of rotational speed needed to match the electric generator.

The present study has been conducted on Siemens Gamesa Renewable Energy 3.X gearboxes manufactured by Gamesa Energy Transmission with a rated power of 3.4MW. These gearboxes have two planetary and one parallel helical gear stage with a total weight of 29.5 ton and input speed of 10.53 rpm. Table 1 shows the number of teeth of each gear in the gearbox and Table 2 gives the gear mesh and shaft rotation excitation frequencies of the gearbox.

Table 1. Teeth numbers of SGRE 3.X 50Hz gearbox.

Gear Stage	Component	Teeth number N
Stage 1	Ring	96
	Planet	35
	Sun	24
Stage 2	Ring	114
	Planet	45
	Sun	21
Stage 3	HSIS	96
	HSS	29

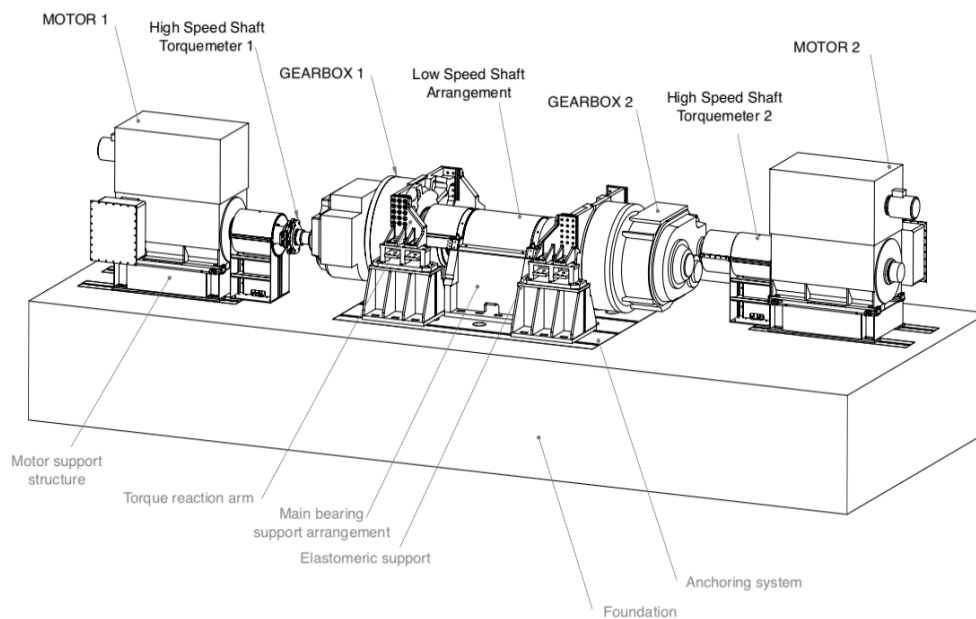### 2.2. Back to back test benches
Wind turbine gearboxes are typically tested in a back-to-back arrangement. Connecting two gearboxes through the low-speed shaft (LSS) enables a cost-effective manner to reproduce the torques generated by wind turbine rotors. Figure 1 shows the standard architecture of a gearbox back-to-back test bench where electric motors produce the driver (action) and driven (reaction) torques. These type of test benches are known as electric as opposed to mechanical variants

Table 2. Rotational and gear mesh frequencies of SGRE 3.X 50Hz gearbox.

	Frequency (Hz)	Order of HSS
HSS	18.6667	1
HSIS (SUN2)	5.6389	0.3021
SUN1 (PC2)	0.8772	0.0470
PC1 (LSS)	0.1754	0.0094
GMF1	16.8414	0.9022
GMF2	5.6389	5.3569
GMF3	541.3333	29

where the input torque is achieved by mechanical means. In the back to back configuration, an additional gearbox is used to increase the torque from the electric motor acting as a driver and reduce the rotating speed, achieving the desired test conditions for the master gearbox.

The main differences between the wind turbine configuration and the back to back test bench are the lack of a tilt angle, the stiffness of the frame supporting the gearbox and the lack of other input excitation besides torque.

Figure 1. Back to back test bench layout.

The torque data used in this study has been gathered by two torque meters placed between the high-speed shaft of the gearboxes and the electric motors in the location shown in Figure 1.

3. Torsional vibration simulation model

A dynamic model of the gearbox for torsional vibration has been derived from first principles based on discrete or lumped parameters. Characteristics such as inertia, elasticity, viscosity and forces have been attributed to concentrated individual elements of the gearbox. The flexibility of gear teeth has been neglected; therefore, the model has been constructed using torsionally

flexible shafts connected with rigid gears. The primary purpose of this model for torsional vibrations is to study stability regions and natural frequencies of the multi-stage gearbox.

The modelling methodology is based on the work published by Girsang et al. in [1]. The model is a linear time-invariant LTI model and has been constructed using Simscape(MATLAB)® [5]. The resulting model is equivalent to deriving a state-space model from differential equations of the lumped elements considered in the system. Within the gearbox all three stages have been considered, each of them with the teeth numbers shown in Table 1; the inertia and stiffness of the components have been calculated using the dimensional drawings and the material properties. The damping coefficients have been estimated using the formulas proposed by Z. Y. Mohammad [6]. The damping ratios used in the model are the mean values of the ranges proposed by [6], that is $\xi_S = 0.04$ for shafts and $\xi_G = 0.1$ for gears. Figure 5 shows the model representation of a single gearbox in Simscape and Figure 3 the resulting magnitude bode diagram form high-speed shaft (HSS) torque to low-speed shaft (LSS) speed. Each of the gear stages gives rise to a resonance frequency as expected from a lumped mass system with four inertias connected by three flexible elements. The stiffness value of the elastomers connecting the torque reaction arms to the mainframe has also been considered in the model. The stiffness value of the elastomers was derived experimentally from displacement measurements at different toque levels.

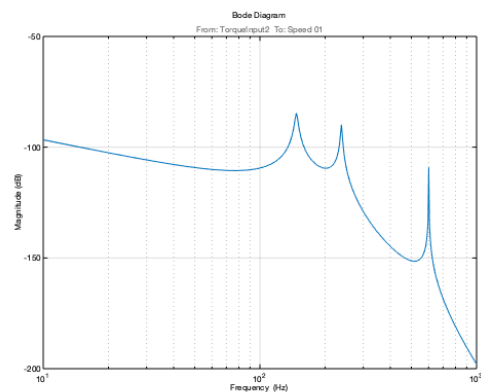**Figure 2.** Lift operation of two gearboxes.

Figure 3. Bode magnitude diagram from HSS torque to LSS speed of a single gearbox.

The model of the gearbox has been extended to study the behaviour of the complete test bench by integrating two gearbox models connected by the low-speed shaft interface through a flexible shaft and adding the stiffness and the inertia of the high-speed shaft couplings to the motors. Connecting the gearboxes in a back to back arrangement and adding the low-speed shaft connection and high-speed shaft couplings has a considerable effect on the dynamic behaviour of the complete system as can be seen in Figure 4.

The complete back to back test bench model has been used to create simulated data of the experiments performed on gearbox prototypes. In order to do so, two PI control loops have been implemented. The input or driver end torque of the test bench is controlled to achieve the reference speed, and the output or driven end torque is controlled to provide the desired braking torque. The proportional and integration constants of the PI controllers have been tuned to achieve a similar response to the one measured in the test bench in terms of rising time and overshoot.

System identification has been applied to simulated torque and rotational speed signals. In total, 4 types of tests have been simulated: two speed-ramps and two torque-ramps. The torque ramps consist of a constant speed reference, W, and equal to the nominal speed (1120 rpm =
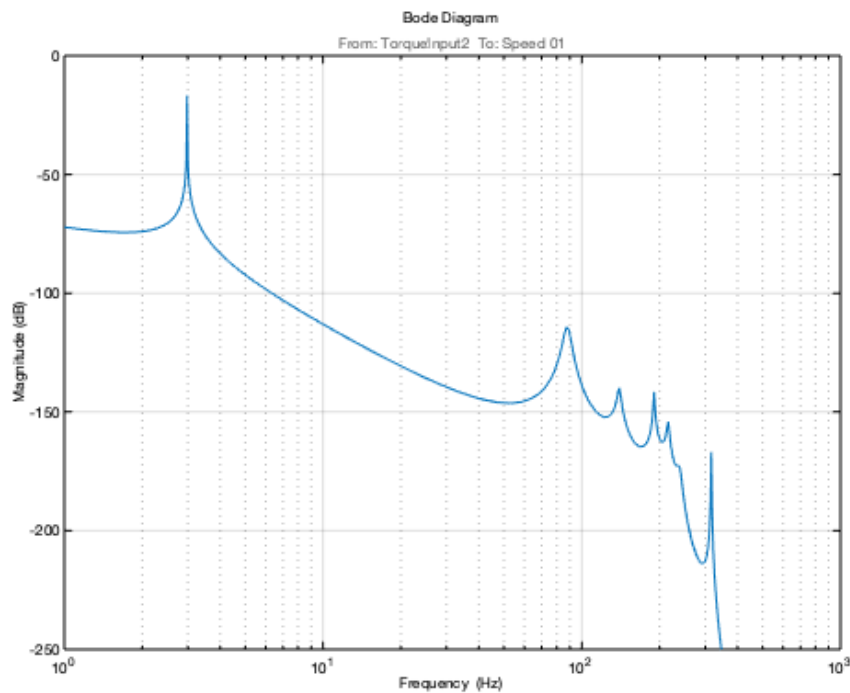
Figure 4. Bode magnitude diagram of the complete back to back test bench model.

117.2861 rad/s) and a torque reference which is changed from an average value of 16.25kNm (50% of the nominal torque) plus and minus 5kNm. On the other hand, during the speed ramps, the torque reference is kept constant (16.25kNm) and the speed is changed from a mean value of 1120rpm up and down 50rpm. For each test case, two options have been studied, the ideal case with square steps and a more realistic case with tapered steps.

Different system identification algorithms have been implemented with a focus on subspace identification methods. The best-fitting model identified from data was found with the square speed ramp sequence, using the driving toque as input and driven speed as output. Using this input-output signal pairing a good match was possible up to around 100Hz Figure 6 with the PBSID algorithm [11]

4. Torque and rotational speed measurements

Experiments have been carried out with two Siemens Gamesa Renewable Energy 3.X gearboxes in a back to back test bench located in the manufacturing plant of Gamesa Energy Transmission of Lerma (Spain). Data of torque signals from the torque meters and the train of pulses from the tachometer probes has been logged during speed and torque ramps sequences defined in Section 3. The location of the sensors is shown in Figure 1.

The performance of the test bench is limited, and an ideal square step cannot be realised. A time constant designated as the ramp time is introduced to the test bench control which tappers the control reference input in a linear way. The ramp time in the test bench is set to 90 seconds both for speed and torque. This ramp time means that for the speed loop the reference takes 90 s to reach the full range of 1980rpm (maximum allowable speed) and for the torque loop the reference takes 90 s to reach the full range of 40kNm (maximum allowable torque).

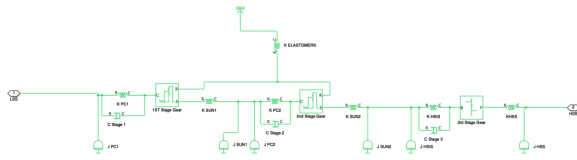Figure 7 shows the measured rotational speed signal vs time during the speed-ramps tests

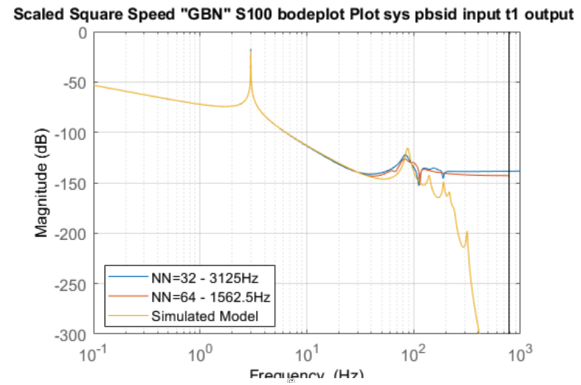**Figure 5.** Simscape model representation of complete Gearbox

Figure 6. Bode magnitude diagram of identified model vs simulation.

performed on gearbox 1, where gearbox 1 is acting as a driven multiplier, and gearbox 2 is acting as the driver reducing gearbox. During the speed-ramps tests, the reference torque is kept constant, and the speed is changed in steps of 50rpm up and down from the average value. Figure 8 shows the evolution of torque during the same seed-ramps test. Plots in Figure 7 and Figure 8 show the torque and speeds measured in the high-speed shafts of both gearboxes (GB1 and GB2). Speed and torque measurements of the torque-ramps tests are shown in Figure 9 and Figure 10.
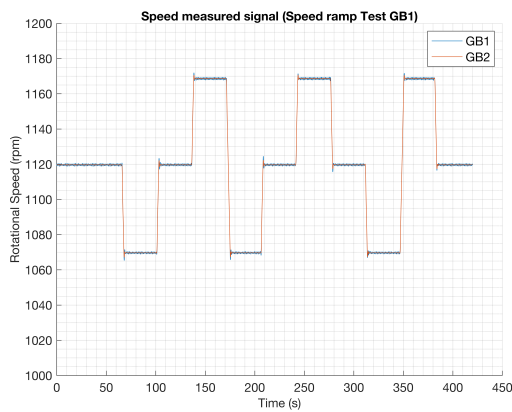

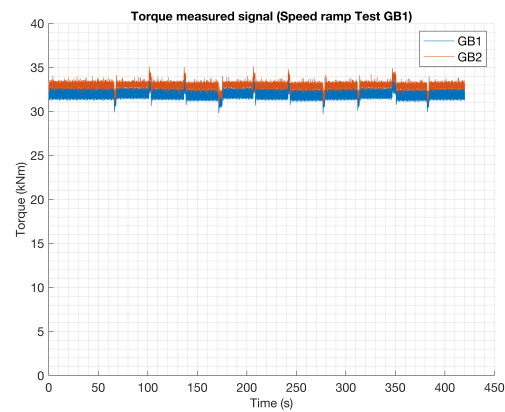**Figure 7.** Rotational speed vs time during speed ramp test on gearbox 1.

Figure 8. Torque vs time during speed ramp test on gearbox 1.

5. Harmonic removal

First attempts to apply system identification algorithms to the torque and speed signals measured in the test bench trials have shown that the power spectra of the signals are much more complex than the simulated counterparts. The frequency content of the signals is dominated by gearbox excitation frequencies such as the shaft rotation and gear mesh frequencies and their harmonics. Gearbox excitation frequencies can be calculated from the relationship of teeth numbers and depend on the rotational speed of the gearbox. The gear mesh frequencies and shaft rotational frequencies of the gearboxes used for the present study can be found in Table 2. In an attempt to separate gear and shaft excitation from structural resonance frequencies in
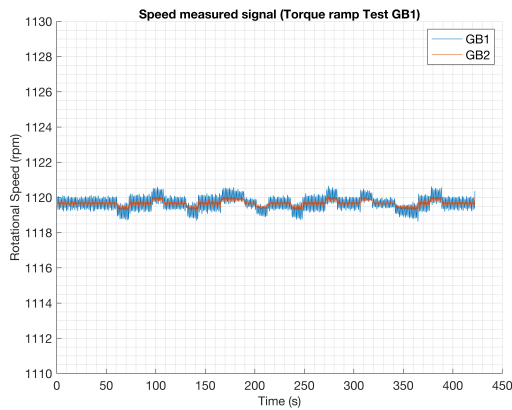
Figure 9. Rotational speed vs time during torque ramp test on gearbox 1.
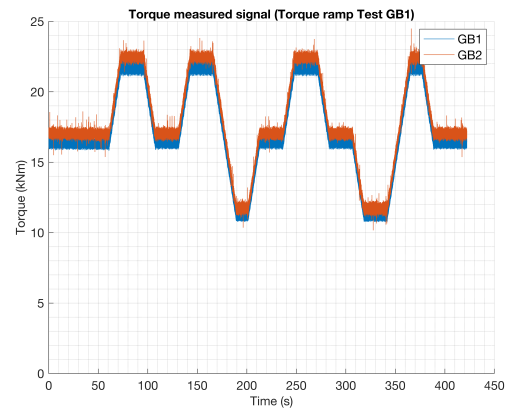

Figure 10. Torque vs time during torque ramp test on gearbox 1.

the gearbox a speed sweep test was performed on the gearboxes. During this test, the torque reference is kept constant and the rotational speed is changed over a wide range, in this case from 400rpm to 1120rpm. Figure 11 shows a waterfall plot of the power spectrum of the torque signal vs rpm of gearbox 1 during the rotational speed sweep test. The power spectrum is dominated by the third harmonic of the running frequency of the high-speed shaft and the second stage gear mesh frequency. Figure 11 also shows the great number of harmonics present in the signal. Gear mesh frequencies, shaft rotational frequencies and their harmonics appear as diagonal lines in the waterfall plot of the power spectrum. Resonance frequencies, on the other hand, are independent of the rotational speed and show up as horizontal lines (fixed frequency). There appears to be a resonance frequency, independent of the rotational speed slightly above 60Hz but the response to this frequency is diluted among all the gearbox excitation frequencies.
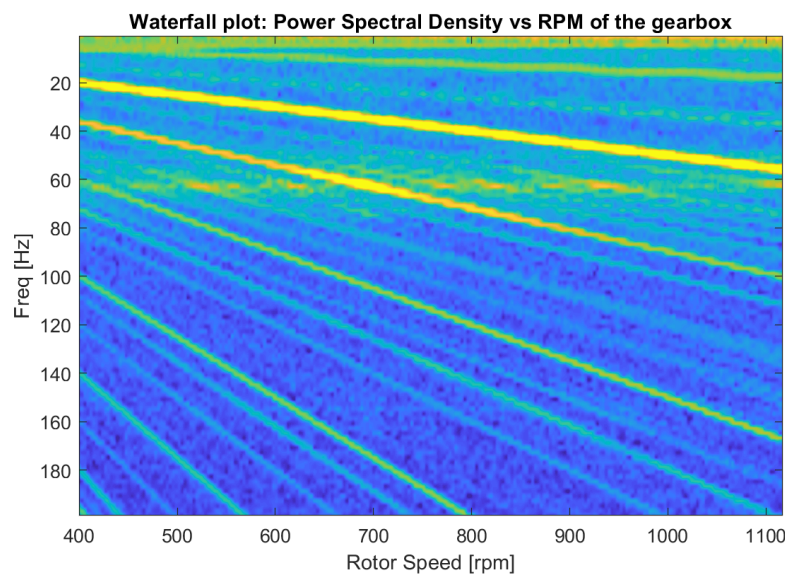

Figure 11. Power spectrum of torque signal (gearbox 1) vs rotational speed

The separation of deterministic and random components of signals related to rotating

7

machinery is a topic that has been studied extensively in the past with two main objectives: improving condition monitoring techniques (i.e. detection of faulty bearings) and in the field of Operational Modal Analysis. Randall et al. reviewed a number of methods for the separation of deterministic and random signals in [8]. The time synchronous averaging (TSA) technique is based on averaging periodic sections of a signal. According to [8] TSA gives minimum disruption of the residual signal and the best separation, but requires an a priori knowledge of the period sought which can be realised by a train of pulses from a tachometer probe. This technique is not suitable for large variations of rotational speed. An alternative method proposed by the software module of Simcenter Testlab (formerly called LMS Test.Lab) [4] has been trialled with the torque signals. In this method, the averaging is done over a number of cycles or revolutions (during the present study, an average of 10 revolutions was performed). The average captures the data synchronous with the selected tachometer. The average is then subtracted from each individual cycle to remove the fundamental frequency and its harmonics. Using the cycle defined by a revolution of the high-speed shaft (using the pulses from the tachometer probe) the results are shown in Figure 12 and Figure 13. A significant reduction of the third order is achieved, but the peak relative to the second gear mesh frequency remains unaltered. The gear mesh frequency of the second stage is 5.3569 times the frequency of the high-speed shaft. Since the relationship is not an integer number time-synchronous averaging does not have any effect on this frequency.
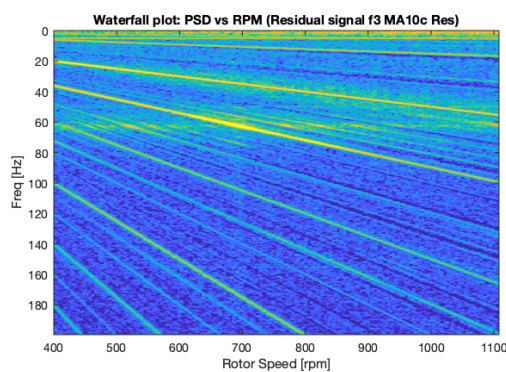

Figure 12. Power spectrum of residual torque signal (gearbox 1) vs rotational speed after applying a 10 high speed shaft cycle averaging .
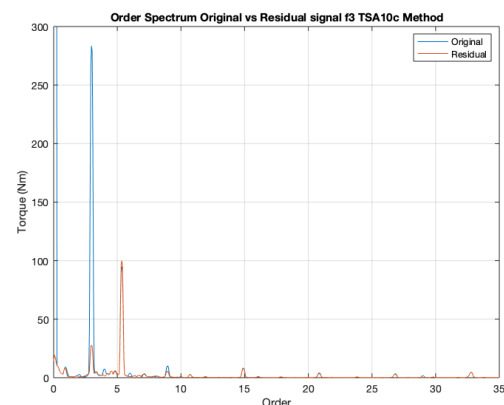

Figure 13. Order spectrum of residual torque signal (gearbox 1) vs rotational speed after applying a 10 high speed shaft cycle averaging .

Some of the harmonic families in the gearbox, like the first or second planetary gear stage mesh frequencies, are not integer multiples of the output speed shaft (Table 2). A separate angular sampling is needed for each harmonic family. Since the only available tachometer probe is located in the high-speed shaft of the gearbox, two alternatives have been studied computing virtual pulses using the known gear ratios from Table 2. On the first alternative a train of pulses corresponding to the second stage gear mesh frequency was created (1 pulse per gear mesh event) and on the second alternative, a train of pulses relative to the speed of the second stage planet carrier (1 pulse per revolution of the carrier). The results are shown in Figure 14 to Figure 17. Synchronising the virtual taco pulses with the mesh events of the gear mesh frequency gives the best removal of the second stage gear mesh order and its harmonics. However, the effect on frequency resolution has to be investigated further. As the averaging period becomes smaller,

the frequency resolution also becomes smaller, and a resonance frequency could potentially be removed by mistake if the separation to the gear mesh frequency is small.
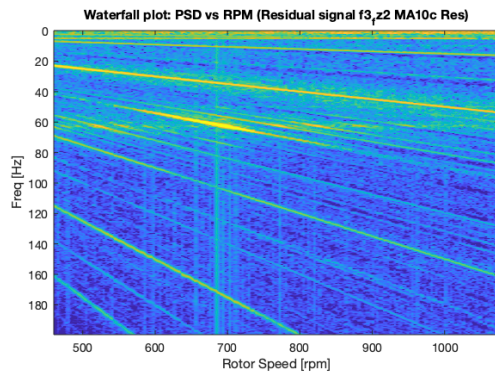

Figure 14. Power spectrum of residual torque signal (gearbox 1) vs rotational speed after applying a 10 planet carrier 2 revolutions averaging .
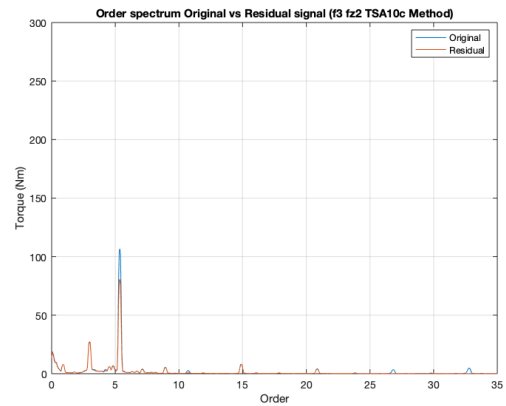

Figure 15. Order spectrum of residual torque signal (gearbox 1) vs rotational speed after applying a 10 planet carrier 2 revolutions averaging .
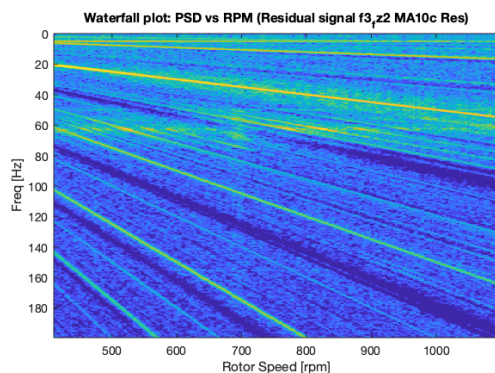

Figure 16. Power spectrum of residual torque signal (gearbox 1) vs rotational speed after applying a 10 second stage gear mesh period averaging .
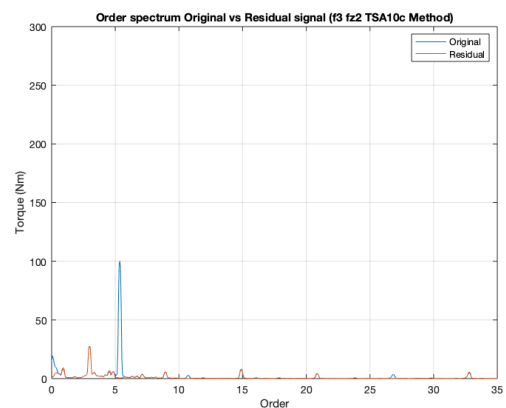

Figure 17. Order spectrum of residual torque signal (gearbox 1) vs rotational speed after applying a 10 second stage gear mesh period averaging .

6. Conclusions

A dynamic torsional model of MW wind turbine gearboxes has been built using first principles based on discrete or lumped parameters (*i.e.* inertia, stiffness and damping). This theoretical model has been combined with the test bench elements to create a model of the complete test bench. Two proportional and integral feedback loops have been implemented to simulate the operation of the test bench. System identification algorithms have been applied successfully to simulated torque and rotational speed signals. The best results have been obtained using predictor-based system identification algorithms on speed ramp test sequences where it was

possible to identify correctly the simulated signal generating model up to 100Hz. Physical experiments have been conducted on a back-to-back gearbox test bench, located at a gearbox manufacturing facility of Siemens Gamesa using two gearboxes of 3.4MW rated power. Gearbox excitation frequencies and their harmonics have been found to dominate the measured signals and disturb the system identification algorithms. Several techniques have been evaluated to separate the deterministic and random components from the experimental torque and rotational speed signals based on time synchronous averaging. Time synchronous averaging captures the data synchronous with the selected tachometer used to define the averaged cycle. The gear mesh frequencies of the planetary stages are not integer multiples of the output high-speed shaft. A train of virtual taco pulses, synchronous with the mesh events of the second planetary stage, has given the best removal of the second stage gear mesh order and its harmonics. However, the disruption of the residual signal and the frequency resolution to separate adjacent frequencies has to be investigated further.

In order to fuse data-driven and physically derived models, the following future research work is proposed:

- Investigate alternative techniques to remove gearbox excitation frequencies
- Apply system identification to filtered signals (signals without gearbox excitation frequency harmonics).
- Find the parameters of the simulation model that best fit the data-driven identified model

References

[1] Irving P. Girsang, Jaspreet S. Dhupia, Eduard Muljadi, Mohit Singh, and Lucy Y. Pao. Gearbox and drivetrain models to study dynamic effects of modern wind turbines. *IEEE Transactions on Industry Applications*, 50(6):3777–3786, 2014.

[2] Jan Helsen, Ben Marrant, Frederik Vanhollebeke, Filip De Coninck, Dries Berckmans, Dirk Vandepitte, and Wim Desmet. Assessment of excitation mechanisms and structural flexibility influence in excitation propagation in multi-megawatt wind turbine gearboxes: Experiments and flexible multibody model optimization. *Mechanical Systems and Signal Processing*, 40(1):114–135, 2013.

[3] Jonathan Keller. Wind Turbine Drivetrain Testing and Research at the National Renewable Energy Laboratory. 2014.

[4] LMS. *Test.Lab 11C User Manual*. LMS International., Leuven, Belgium, 2011.

[5] MATLAB. *version 9.7.0 (R2019b)*. The MathWorks Inc., Natick, Massachusetts, 2019.

[6] Z Y Mohammad. Estimation of Model Parameters , for Torsional Vibration Analysis of a Turbo-Generator Unit with Reference to Mosul Gas-Turbine Station. pages 10–11, 2014.

[7] JLM Peeters and D Vandepitte. Structural analysis of a wind turbine and its drive train using the flexible multibody simulation technique. *Proceedings of ISMA*, (January 2006):3665–3680, 2006.

[8] R B Randall, N Sawalhi, and M Coats. A comparison of methods for separation of deterministic and random signals. *International Journal of Condition Monitoring*, 1(1):11–19, 2011.

[9] Brian Resor, David Wilson, Thanasis Barlas, Dale Berg, and Gijs van Kuik. Active Aerodynamic Blade Distributed Flap Control Design Proceedure for Load Reduction on the UPWIND 5MW Wind Turbine. (January), 2013.

[10] S. Struggl, V. Berbyuk, and H. Johansson. Review on wind turbines with focus on drive train system dynamics. *Wind Energy*, 18(4):567–590, apr 2015.

[11] Gijs van der Veen, Jan-Willem van Wingerden, Marco Bergamasco, Marco Lovera, and Michel Verhaegen. Closed-loop subspace identification methods: an overview. *IET Control Theory Applications*, 7:1339–1358(19), July 2013.

[12] G. A. M. van Kuik, P. E. Morthorst, D. Matha, M. Muskulus, P. Tavner, D. Schlipf, A. Abrahamsen, J. W. van Wingerden, R. Nijssen, J. Mann, D. Lekou, S. Lehnhoff, S. Degraer, P. E. Sørensen, R. W. Künneke, P. Gebraad, C. L. Bottasso, J. D. Sørensen, J. N. Sørensen, K. Skytte, G. J. W. van Bussel, H. J. Lindeboom, O. Kramer, H. Polinder, J. Peinke, M. Sonnenschein, and C. Ferreira. Long-term research challenges in wind energy – a research agenda by the European Academy of Wind Energy. *Wind Energy Science*, 1(1):1–39, 2016.